Space-Charge Effects in the Cyclotron-resonance Laser Accelerator[*]

R. Pakter[a], I.L. Caldas[a], F. Couto[b], T.S. Caetano[b], and F.B. Rizzato[b]
[a] Instituto de Física – Universidade de São Paulo
[b] Instituto de Física – Universidade Federal do Rio Grande do Sul

Abstract

In this work, we analyze the effects produced by the inclusion of space-charge waves in a Hamiltonian model for a cyclotron resonant accelerator. We find that space-charges impose limits on acceleration and that these limits appear as bounding curves on the appropriate stroboscopic phase-spaces. In addition, space-charges create nonlinearly locked states which undergo not only the period doubling bifurcations preceding chaos, but saddle-node inverse bifurcations as well.

1 INTRODUCTION

A promising configuration for laser acceleration of charged particles is the so called cyclotron-resonance accelerator, where a coherent electromagnetic wave may transfer a large amount of energy to a beam of electrons gyrating in a guide magnetic field [1, 2].

Transverse space-charge effects are usually believed to be of lesser importance in cyclotron accelerators because the related fields tend to be small if the particle beam is of appropriate thickness [2]. As for longitudinal space-charge effects along the accelerating length the situation is a little different. In fact, if one works with powerful microwave sources for which the vector potential of the electromagnetic field is large, velocity gradients along the acceleration length can grow to such magnitude that beam bunching and the corresponding space-charges may become appreciable.

Our intention here is to analyze the longitudinal space-charge effects originated from velocity gradients.

2 THE MODEL

Let us assume that our system operates in a steady-state fashion. Therefore, what one actually has is a beam of electrons which is continuously injected into some accelerating region lying along a magnetized, say, z axis which we call the longitudinal axis. We further assume that the potential vector of the electromagnetic wave field is written as $-\frac{|e|}{mc^2}\mathbf{A}(z) = A\left[-\hat{\mathbf{x}}\cos(kz - \omega t) + \hat{\mathbf{y}}\sin(kz - \omega t)\right]$, with

$$A = \begin{cases} 0, & \text{if } z < 0 \\ \sqrt{\rho}, & \text{if } z > 0, \end{cases} \qquad (1)$$

where ρ is an adimensional constant factor determining the field amplitude, k is the wave vector and ω is the wave frequency. Relation (1) means that the accelerating region lies on the half-space $z > 0$. A beam of particles is incident from the far left, $z < 0$, with an initial velocity $v_o \equiv \lim_{z \to -\infty} v_z$ where v_z is z-component of the particle velocity.

In previous papers a variety of alternatives have been presented to compensate the limiting effects imposed by the dispersion naturally found in real systems [3, 4]. Therefore, considering that these effects can be cured, here we shall focus only on space-charge effects, assuming $\omega/k = c$ throughout.

The adimensional Hamiltonian H describing the temporal dynamics of an individual particle is then written in the form [4]

$$\begin{aligned} H &= -\omega I - \phi \\ &+ \sqrt{1 + 2I + (P_z + \omega I)^2 + 2\sqrt{2\rho I}\cos\theta + \rho} \end{aligned} \qquad (2)$$

where P_z is the canonical momentum related to the kinetic momentum p_z by $p_z = P_z + \omega I$, and where we include the adimensional electrostatic potential $\phi = \frac{|e|\phi_{dimensional}}{mc^2}$. The relativistic factor γ is precisely given by $\gamma = H + \omega I + \phi$, the pair (I, θ) is a canonical action-angle pair describing the transverse motion, and the frequency ω is normalized with respect to Ω_c. Since the system is time independent, H is a constant. Thus it proves convenient to reconstruct the Hamiltonian formalism so as to have the coordinate z playing the role of time. The receipt to carry out the transformation is known [5]; it suffices to invert relation (3) writing

$$P_z = P_z(I, \theta, \phi), \qquad (3)$$

where the positive signal of the square root is chosen so as to represent rightward moving particles. Dynamical equations are obtained from

$$d_z\theta = \partial_I(-P_z) \quad \text{and} \quad d_zI = -\partial_\theta(-P_z). \qquad (4)$$

The purpose of the present investigation is to augment the previous equations with the appropriate Poisson equation for electrostatic potential ϕ of the space-charge field. We assume in this paper that the longitudinal bunching resulting from longitudinal gradients is sufficiently intense that we can disregard transversal derivatives in the equation for ϕ. This approximation works well whenever the system has no transverse bounds, as in magnetospheric systems, as well as when in laboratory schemes the wave frequency is such that

$\omega \gg 10$ GHz. In this regard, we mention that the microwave regime of present accelerators uses frequencies on the order of $10\,GHz$ while optical and millimetric accelerators are expected to work with much higher frequencies. Anyway, we expect our approximations to provide qualitative true results, especially on the existence, shape and significance of limiting curves, and on the occurrence and types of bifurcations. Poisson equation can then be casted in the form

$$d_z^2 \phi = n(z) - n_o, \qquad (5)$$

where particle density is normalized to $\frac{\Omega_c^2 mc}{4\pi|e|}$, n_o stands for the unperturbed density of the beam prior its entrance into the accelerating region $z > 0$ and references to perpendicular coordinates are no longer present due to and average taken over the cross section of the system. We assume that at $z = 0$ all the particles are injected into the accelerating region with the same action I and gyrophase angle θ, that is consistent with the nonadiabatic phase bunching which occurs in this kind of system when particles are injected with small values of I [4], a condition assumed throughout the text. With these hypothesis in mind one can use continuity equation along z axis to see that $n(z) = \lambda v_o / v_z(z)$, where the parameter $\lambda = \frac{4\pi|e|n_o}{\Omega_c^2 mc}$ is a measure of the unperturbed beam density; as usual, we consider beams for which $\lambda \ll 1$.

In summary, we have four first-order nonlinearly coupled equations to solve. Two of them, Eqs. (4), describe action-angle dynamics and the remaining two, obtainable from Eq. (5) as

$$d_z \phi = \lambda v_o \mathcal{E}(z) \quad \text{and} \quad d_z \mathcal{E} = v_z(z)^{-1} - v_o^{-1}, \quad (6)$$

describe the space-charges induced by the bunched longitudinal dynamics. As seen, the action-angle equations are derived from a Hamiltonian principle. It turns out that Eqs. (6) can be also seen as a canonical pair if Hamiltonian (3) is conveniently extended to

$$\mathcal{P}_z(I, \theta, \mathcal{E}, \phi) \equiv P_z(I, \theta, \phi) - \lambda v_o \mathcal{E}^2/2 - \phi/v_o. \quad (7)$$

Now, $\mathcal{E}$ and ϕ are canonically conjugated momentum and coordinate whose dynamics is derived from

$$d_z \mathcal{E} = -\partial_\phi(-\mathcal{P}_z) \quad \text{and} \quad d_z \phi = \partial_\mathcal{E}(-\mathcal{P}_z). \quad (8)$$

$\mathcal{P}_z$ is not explicitly dependent on z as long as one does not go through $z = 0$ where ρ undergoes its jump. The constant values of $\mathcal{P}_z$ on both sides of $z = 0$ are (assuming for $z < 0$: $I \sim 0$, $\phi = \mathcal{E} = 0$)

$$\mathcal{P}_z = \begin{cases} \sqrt{H^2 - 1}, & \text{if } z < 0 \\ \sqrt{H^2 - 1 - \rho}, & \text{if } z > 0, \end{cases} \quad (9)$$

where $H = (1 - v_o^2)^{-1/2}$. In particular, it is seen that only particles with $v_o^2 > \frac{\rho}{1+\rho}$ can be injected into the region $z > 0$.

Figure 1   Figure 2
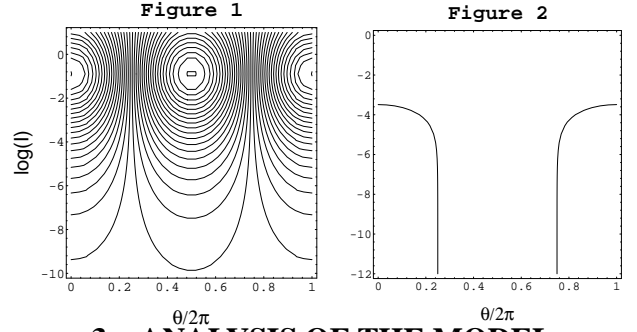
3 ANALYSIS OF THE MODEL

3.1 General aspects

Let us first briefly see how the system behaves when electrostatic effects are turned off. For this situation where the governing Hamiltonian is simply P_z, Eq. (3), the associated phase-space is shown in Fig. (1). The figure reveals the existence of two elliptic fixed points whose respective trapping regions are isolated from each other by straight lines at $\theta = \pi/2, 3\pi/2$. Particles launched near $\theta = \pi/2$ or with $I \ll 1$ naturally undergo enormous acceleration as times advances. Inhibiting effects appears when the space-charge wave is turned on. In this case the complete Hamiltonian $\mathcal{P}_z$ is to be used. As this Hamiltonian is 2-degrees-of-freedom, stroboscopic maps come in order. We choose to plot the pair (I, θ) each time $\mathcal{E} = 0$ with $d_z \mathcal{E} > 0$. One relevant feature associated with our stroboscopic maps is the fact that they give rise to the appearance of limiting curves [6] that separates forbidden from allowed regions on the phase-space. These curves can be determined based on the fact that $\mathcal{P}_x$ is a constant of motion. Their form is depicted in Fig. (2) and the possible dynamics on the stroboscopic plane develops above it. Note that for $\pi/2 < \theta < 3\pi/2$ the corresponding I vanishes. We will be mostly interested in particles injected with as low as possible initial transverse energy, which means particles whose first piercing through the stroboscopic plane is located close to the limiting curve, at $I \ll 1$. The importance of limiting curves, is that they are KAM curves to which those low energy particles stick as far as the motion is integrable there. Therefore, if a particle is launched near the limiting curve, it tends to stay near it as long as the curve is not destroyed by cascade of period doubling and chaos. Considering this feature, one can readily determine the maximum I-excursion merely by inspecting the maximum value of I along the curve. For small values of ρ, a simple analysis yields $I_{max} \sim 2\,\rho^{1/3}$.

3.2 Nonlinear analysis

Let us now proceed to the full nonlinear analysis considering $v_o = 0.7$ and $\lambda = 0.01$ since these values prove to be fairly realistic both in laboratory and magnetospheric environments. Focusing attention on stroboscopic plots first, the initial conditions are to be chosen so as to satisfy the second relation of Eq. (9). In general we launch particles with $\theta = \pi$, with $\mathcal{E} = 0$, with various values of I

- initial values are denoted by I_o - and with ϕ calculated from the conserved Hamiltonian. In Fig. (3a) the phase-space is shown for $\rho = 3.5 \times 10^{-6}$. At this particular value of the wave amplitude, the phase flux is distorted in two ways. The first is connected with the appearance of the limiting curve inhibiting unbounded acceleration; the other, is the occurrence of phase-locked states which appear as resonant nonlinear islands in the plots [7]. Resonant islands are the first real symptoms of nonintegrability. As it appears, they are formed as a result of the nonlinear resonance involving two typical frequencies of the system: the plasma frequency with which the density would fluctuate if the cyclotron resonance interaction were turned off and the cyclotron modulation frequency, which results from the periodic energy exchange between particles and laser. For the parameters used in the paper, the cyclotron modulation frequency, ω_{cm}, is smaller than the plasma frequency, ω_e. This suggests that the principal type of resonance could be written in the form $p\omega_{cm} = \omega_e$, where p is an integer yielding the number of islands in the particular p-resonance chain. In Fig. (3a) one can see the $p = 4, 3, 2$ islands from bottom to top. From the figure, one is lead to think that the closer the resonant chain is to the limiting curve, the smaller is the frequency ratio $\frac{\omega_{cm}}{\omega_e}$. This proves to be true only up to a certain extent. To examine this question in more detail, we make use of the numerically calculated winding number, that is a direct measure of above frequency ratio. The complete winding curve is constructed for several initial conditions and is shown in Fig. (3b). The figure reveals that the winding actually is a nonmonotonic function which grows for relatively large values of I_o, but decreases if I_o is very small. This nonmonotonicity of the winding curve has been detected in a variety of problems associated with accelerator physics [8, 9] and implies an interesting result. The result is that at a certain point, a resonance located on the right side of the minimum of the W-curve can collapse against another resonance, with the same winding, but located on the left side of the minimum. This kind of bifurcation is called inverse saddle-node bifurcation. The resonances along a winding curve appear in the form of small plateaus. In Fig. (3b) the resonances $p = 4$ and $p = 2$ can be clearly devised on the right side of the minimum. The absence of relatively large plateaus at expected positions, like at $W = 1/3$, does not mean that the corresponding resonance is absent; it merely indicates that initial conditions were launched across an hyperbolic point of the island, where the local resonance width effectively vanishes.

Returning to the analysis of bifurcations, we note that in relatively more usual cases, winding curves of low-dimensional Hamiltonian systems are monotonic and only period doubling bifurcations are possible. In the present situation the possibility exists of saddle-nodes as well. We found that If a resonance has not been destroyed yet and is very close to the minimum of the winding curve, as ρ is increased, a saddle-node bifurcation occur before any period doubling (this is the case for the $p = 4$ resonance

Figure 3a

Figure 3b
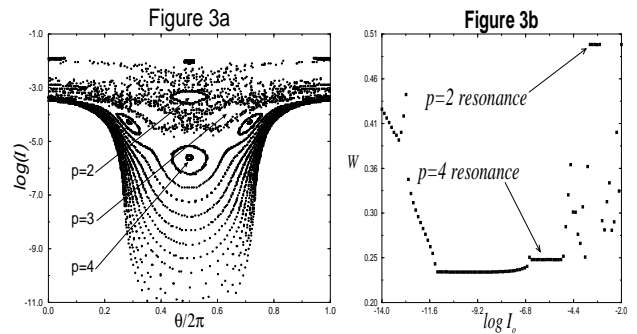
shown). On the other hand, deep inside the monotonically increasing or decreasing sections of the winding curve the predominant type of bifurcation is of the period doubling type (which is the case for the $p = 2$ resonance shown).

While the chaotic portion of the phase-space keeps away from the limiting curve, the acceleration can be expected to be regular, since particle injected close to the curve tend to stay near the curve. Only when the value of ρ is large, the chaotic portion arrives at the limiting curve, dragging the particles into this stochastic sea. From these comments one sees that the wave amplitude cannot be increased forever in order to improve regular acceleration. For $\lambda = 0.01$ and $v_o = 0.7$, we found that chaos arrives at the limiting curve when $\sqrt{\rho} \sim 0.02$; in particular, this results in $\gamma_{max} \sim 2.0$.

4 REFERENCES

[1] P. Sprangle, L. Vlahos, and C.M. Tang, IEEE Trans. Nucl. Sci. **NS-30**, 3177 (1983).

[2] A. Loeb and L. Friedland, Phys. Rev. A **33**, 1828 (1986).

[3] C. Chen, Phys. Rev. A **46**, 6654 (1992).

[4] R. Pakter, R.S. Schneider, and F.B. Rizzato, Phys. Rev. E **49**, 1594 (1994); R. Pakter, F. Couto, and F.B. Rizzato, Phys. Rev. E **52** 4793 (1995).

[5] N.M. Kroll, P.L. Morton, and M.N. Rosenbluth, IEEE Journal of Quantum Electronics **QE-17**, 1436 (1981).

[6] G. Polymilis and K. Hyzanidis, Phys. Rev. E **47**, 4381 (1993).

[7] A.J. Lichtenberg and M.A. Lieberman, *Regular and Stochastic Motion*, Springer (1983).

[8] G. Corso and F.B. Rizzato, Physica D **80**, 296 (1995); Phys. Rev. E **52**, 3591 (1995).

[9] G.A. Oda and I.L. Caldas, Chaos, Solitons & Fractals, **5** 15 (1995).